Robust Class-I BME Ceramic Capacitors for High Temperature Applications

Tim Hollander, Travis Ashburn, Abhijit Gurav, Xilin Xu and Jim Magee
KEMET Electronics Corporation
2835 KEMET Way, Simpsonville, SC 29681
Tel: +01-864-963-6300, Fax: +01-864-963-6492, e-mail: TimHollander@kemet.com

Abstract

In capacitors for applications at temperatures of 150°C or above, such as automotive under-the-hood electronics and power electronics, a robust dielectric material is necessary. In traditional X8R ceramic capacitors (EIA specification, ΔC/C within ±15% between −55°C and +150°C compared that at 25°C), the dielectric material is designed for applications up to 150°C. However, at temperatures above 150°C, the X8R capacitors typically suffer from degradation of reliability performance and severe reduction in capacitance, especially under DC bias conditions. Recently, a Class-I C0G dielectric has been developed using Nickel electrodes for high temperature application up to 200°C. Due to its linear dielectric nature, this material exhibits highly stable capacitance as a function of temperature and voltage. Multilayer Ceramic Capacitors (MLCC) made from this material can be qualified as X9G with robust reliability. This paper will report electrical properties and reliability test data on these Class-I C0G ceramic capacitors at temperatures ≥150°C. In addition, test data from *D-E* curves and energy density measurements will be reported along with a discussion of possible mechanisms behind the robust reliability of this material.

1. Introduction

For applications in harsh environment conditions, such as down-hole oil exploration, automotive under the hood electronics, military devices and avionics, etc., the maximum operating temperature can be much higher than 125°C. These industries need capacitors that are robust and reliable at temperatures in the range of 150°C to 200°C, or even higher. However, at these temperatures, dielectric materials either have significant capacitance variation with temperature, or exhibit high dielectric losses, and hence, are not commonly available in the market [1-4]. Commercial C0G and X7R dielectrics are usually designed for applications up to 125°C, while X8R dielectric is designed for applications up to 150°C. One approach for using the X7R/X8R dielectric at temperatures above their design limit of temperature is by de-rating their rated voltages due to reliability concerns. For example, some X7R dielectrics can be used at 150°C after 50% voltage de-rating [5]. Similarly, it may be possible to use some X8R capacitors at temperatures above 150°C by appropriate voltage de-rating.

One commercially available solution for high temperature applications is KEMET's base-metal electrode (BME) C0G MLCC. This BME C0G typically uses a $CaZrO_3$-based linear dielectric material. Compared to Class-II dielectrics such as the X7R/X5R/X8R materials, the C0G dielectrics have the advantages of high stability of capacitance over temperature and voltage, no aging of capacitance, no micro-phonic effects, and low dielectric loss (*DF*). In addition, with the progress in BME technology, the maximum capacitance offering as well as reliability of this BME C0G is greatly improved compared to the traditional precious metal electrode (PME) C0G MLCC [6-7].

This paper will demonstrate the performance of BME C0G MLCC at temperatures up to 200°C and compare it with PME C0G or X8R based MLCCs. Furthermore, test data from *D-E* curves and energy density will be reported along with discussion of possible mechanisms behind the robust reliability of these BME C0G MLCCs.

2. Materials Characterization

2.1. D-E Curve

From the materials standpoint, since the BME C0G dielectric is a $CaZrO_3$ based linear dielectric, it is intrinsically suitable for high temperature applications. The relations between the electric displacement *D* and electric field *E* (*D*-*E* curve or *D*-*E* loop) were characterized using an automated polarization measurement system. A Polyphenylene Sulphide (PPS) based film capacitor sample with the same capacitance of 100 nF was used for comparison. The *D*-*E* curves measured at room temperature and 170°C are shown in Fig. 1 (a) and (b), respectively.

From room temperature to 170°C, the *D*-*E* curves of the BME C0G dielectric keeps its linear characteristic very well, while the film dielectric shows an obvious widening of the loop due to space charge effects at high temperature. The area of the *D*-*E* loop is proportional to the energy loss in one field sweep cycle. This also indicates that the BME C0G dielectric will have low losses at high temperature than the PPS based film dielectric material. Since $D = \varepsilon_0 * k * E$, the dielectric constant *k* can be calculated from the slope of the *D*-*E* curve. In Fig. 1 (a) and (b), the slopes for C0G MLCC are found to be almost the same and the dielectric constant is calculated to be 32.6. This is the intrinsic reason why the dielectric constant of the BME C0G material is extremely stable with temperatures.

2.2. Energy Density

The amount of energy that can be stored in the BME C0G MLCC at high temperatures was also estimated. The energy density can be expressed in the following format:

$$U_e = \frac{1}{2}\varepsilon_0 k\left(\frac{V}{t}\right)^2 \quad (1)$$

where U_e is the volumetric energy density, ε_0 is the dielectric permittivity of free space (8.85×10^{-12} F/m), *k* is the relative dielectric constant, *V* is the applied bias voltage, and *t* is the dielectric thickness. Equation (1) indicates that the energy density is directly proportional to the dielectric constant, *k* and/or dielectric breakdown strength capability. It is important to note that for non-linear dielectric materials such as the ferroelectric dielectrics, *k* will decrease strongly with increasing voltage and/or temperatures. Further, the maximum voltages that can be applied to the ferroelectric material will also be greatly limited at high temperatures due to the significant drop in its insulation resistance. In contrast, for linear dielectrics, as the dielectric constant, *k,* is constant with voltage at a given temperature, the energy density is proportional to the square of the bias field (*V*/*t*).

From the *D*-*E* curve, the energy density U_e of a dielectric material can also be calculated by integrating $U_e = \int E \bullet d\mathrm{D}$. The energy densities determined from the *D*-*E* curves measured at temperatures of 20°C, 200°C and 300°C for BME C0G 1206/100nF/25V MLCC are plotted in Fig. 2. It is easy to see that the energy density is stable with temperature. Even at 300°C and up to 400V DC bias (or 1429 kV/cm bias field), the BME C0G MLCC still held the energy very well and showed no reduction in capability for energy density (or storage) compared to that at 20°C. At 300°C, dielectric breakdown occurred at bias only above 400V. At 200°C and 500V DC bias which corresponds to a bias field of 1786 kV/cm, the energy density is 4.8 J/cm^3. The typical energy densities reported for ferroelectric or anti-ferroelectric based material were 8 J/cm^3 [8] and 4.9 J/cm^3 [9], respectively. However, these data was obtained from measurements at room temperature. At elevated temperatures, energy densities for these non-linear materials usually fall sharply due to reasons described above. This confirms that the BME C0G material has very good potential to be used in energy storage applications at temperatures above 150°C.

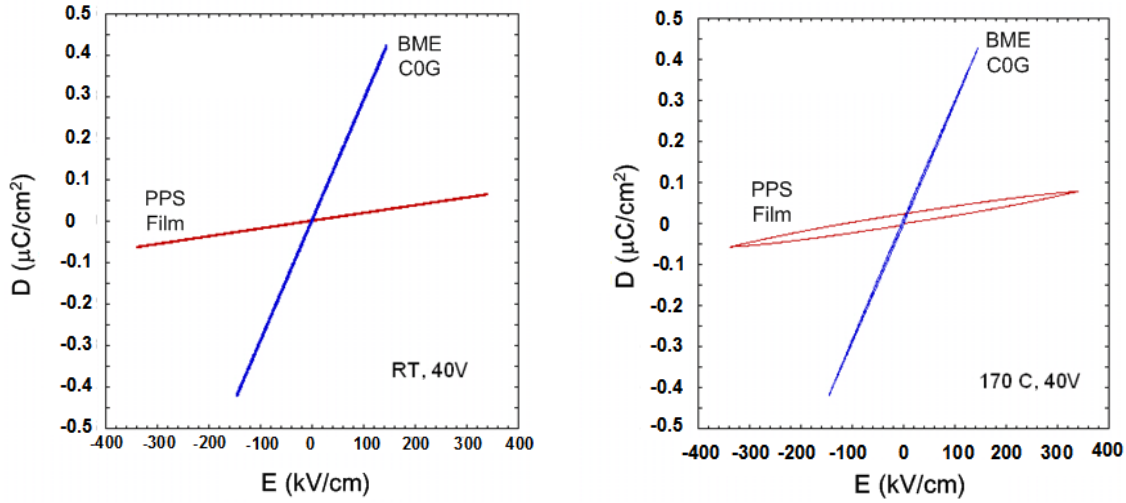

(a) (b)

Fig. 1. *D-E* curves for BME C0G 1206/100nF/25V and 100nF PPS Film Capacitor at (a) 25°C, and (b) 170°C.

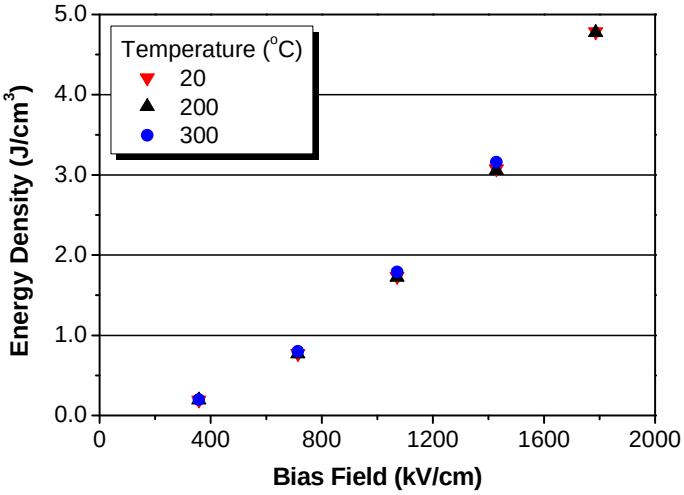

Fig. 2. Energy density of BME C0G 1206/100nF/rated 25V at various temperatures.

3. Electrical Performance at High Temperatures

3.1. BME C0G MLCC vs. PME C0G MLCC

Traditional C0G dielectric materials are mainly based on the barium neodymium titanate (BNT) and are compatible with precious metal electrodes (PME) such as Pd or Ag/Pd. To provide a more cost effective solution, the MLCC manufacturers have mostly converted from PME to BME (mainly Ni electrodes). The BNT material has a dielectric constant (k) of ~70, while the k of $CaZrO_3$-based BME C0G material is ~32. Although the BME-C0G system has a lower dielectric constant, due to the advancement of materials and processing technologies, the BME-C0G materials can be processed into MLCC with higher layer counts and thinner layers. Thus, we are able to use thinner layers of $CaZrO_3$-based materials compared to BNT, and still obtain higher insulation resistance (IR) and better reliability [6, 7]. Hence, for the same case size and voltage rating, BME C0G can offer much higher capacitance than PME because of its thinner, but high reliability dielectric layers [10]. For example, the Highly Accelerated Life Test (HALT) reliability of two 1206 case size 10nF MLCC samples (one is PME C0G and the other is BME C0G) is

shown in Fig. 3. The dielectric thickness for the BME C0G MLCC is 7.0 µm, and that for the PME C0G is 11.6 µm. These two samples both passed the required QA life test, which was performed at 125°C and twice rated voltage for 1000 hours. In order to make these parts fail, the HALT test was conducted at 175°C and 400V. Figure 3 shows that the BME 1206/10nF sample exhibits markedly longer time-to-failure (TTF) values compared to the PME version. The median time-to-failure (MTTF) at HALT for PME 1206/10nF was 62.6 minutes, while that for the BME1206/10nF was 869.6 minutes, which is more than an order of magnitude of improvement in MTTF. This HALT result indicates that BME C0G will be a better material for high temperature applications than PME C0G. The topic of reliability of BME-C0G is discussed further in a later section on lifetime prediction study.

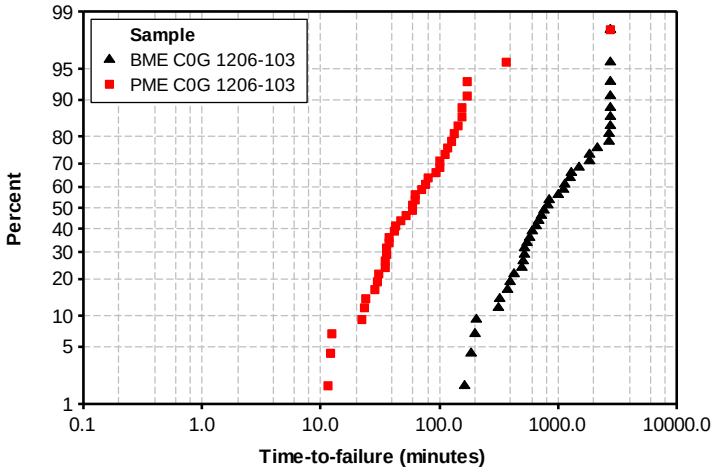

Fig. 3. HALT for PME and BME C0G 1206/10nF MLCCs. (HALT was run at 175°C and 400V.)

The insulation resistance (IR) of these two samples of C0G1206/10nF were also measured in the temperature range of −55°C to +200°C under a DC bias of 25V, and are plotted in Fig. 4. Even with a much thinner dielectric thickness, the BME C0G typically shows higher IR than the PME C0G in the whole temperature range, especially at temperature above 120°C. Due to its special composition and formulation, the IR of the BME C0G started to increase beyond 120°C (instead of decreasing), which resulted in more than two orders of magnitude higher IR than that of the PME C0G at 200°C. This contributes to the robust reliability of the BME C0G at high temperatures.

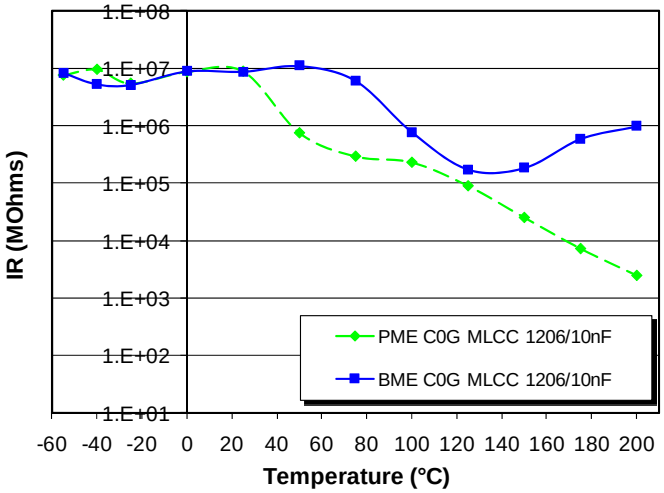

Fig. 4. IR dependence on temperature with 25V DC bias for PME and BME C0G MLCC.

3.2. BME C0G MLCC vs. X8R MLCC

The samples used for comparison are KEMET BME C0G MLCC (1206 case size, 100nF & 25V rated) and a commercially available X8R MLCC (1206 case size, 220nF & 50V rated). The dielectric thickness for the BME C0G MLCC was 2.8 µm, and that for the X8R MLCC was 11.2 µm, which is nearly four times thicker than the BME C0G MLCC.

Figure 5 shows the relative capacitance variation with reference capacitance at 25°C (ΔC/C) versus temperature for BME C0G MLCC and X8R MLCC in the temperature range of −55°C to +200°C. The BME C0G MLCC exhibit extremely flat response over the whole temperature range whether with 25V DC bias applied or without any DC bias. The maximum temperature coefficient of capacitance (TCC) from −55°C to +200°C is found to be 13.4 ppm/°C, which indicates that this dielectric material is not only compliant with the EIA C0G specification, but also can be extended to the X9G specification (capacitance variation from the reference point of 25°C should be within 0 ± 30 ppm/°C (or $\Delta C_{Max}/C \leq 0.525\%$) over the temperature range of −55°C to +200°C). The X8R MLCC hold their capacitance reasonably well below 125°C. However, at temperatures above 125°C, their capacitance decreased sharply. This is because at temperatures above the Curie point (125°C for $BaTiO_3$-based materials), the capacitance (C)–temperature (T) dependence for ferroelectric material follows the Curie-Weiss Law: $C \propto k \propto \Theta/(T\text{-}T_c)$, where k is the dielectric constant, Θ is the Curie constant, and T_c is the Curie temperature. At 200°C, the capacitance of X8R MLCC dropped by 50.1% without DC bias, and by 52.1% while under 25V DC bias compared to their capacitance at 25°C. Hence, the 220 nF X8R MLCC had almost the same effective capacitance at 200°C as the 100 nF BME C0G MLCC. One can also expect that at temperatures above 200°C, the capacitance of the X8R MLCC will reduce to values lower than 100 nF. Thus, for high temperature applications, the actual capacitance under the use conditions needs a serious consideration because of the severe capacitance reduction with temperature (versus considering only the nominal capacitance value at room temperature). Another factor to note is that the actual electric field applied in the BME C0G MLCC was almost 4 times higher than that for the X8R MLCC because of the dielectric thickness difference. If the X8R MLCC were under the same field strength as the BME C0G MLCC, their effective capacitance would have been even lower.

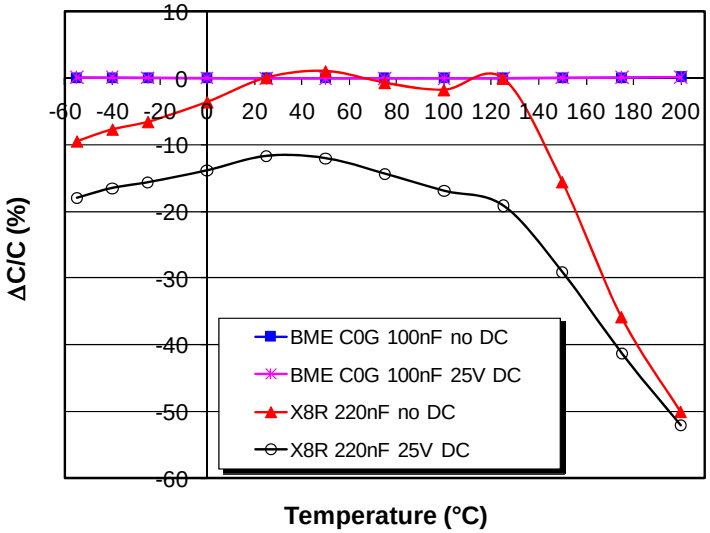

Fig. 5. ΔC/C variation with temperature and DC bias.

The measured dielectric loss or dissipation factor (*DF*) of the BME C0G and X8R MLCC samples without DC bias in the temperature range of −55°C to +200°C is shown in Fig. 6. The BME C0G MLCC has a maximum *DF* of 0.016% over the temperature range investigated. Such extreme low dielectric loss is in good agreement with the *D-E* curve analysis, which showed almost zero loop area at high temperatures. The *DF* of the X8R MLCC was 2.04%

at 25°C and decreased with increasing temperature because of the easier rotation of ferroelectric domains at increasing temperatures. However, the X8R MLCC still showed a *DF* of 0.87% at 200°C.

The comparison of insulation resistance (IR) was quite revealing between the BME C0G and X8R MLCC, as shown in Fig. 7. From room temperature to 200°C, the IR of BME C0G MLCC measured at 25V changed from 1.22 TΩs to 28.3 GΩs. The X8R MLCC sample used in this study was originally rated at 50V for applications below 150°C. In these IR measurements, a voltage of only 25V DC was applied. Even then, the IR of X8R MLCC decreased more than 3 orders of magnitude to 6.3 MΩs at 200°C. This results in an R*C product (capacitance times IR) of only 0.67 MΩ•µF at 200°C, which will be of great concern for the majority of high temperature applications. Thus, the X8R MLCC would need to be de-rated in voltage rating for high temperature applications above 150°C, while the BME C0G capacitors are expected to hold their capacitance, *DF* as well as IR reasonably well over the temperature range of −55°C to +200°C as shown in this study.

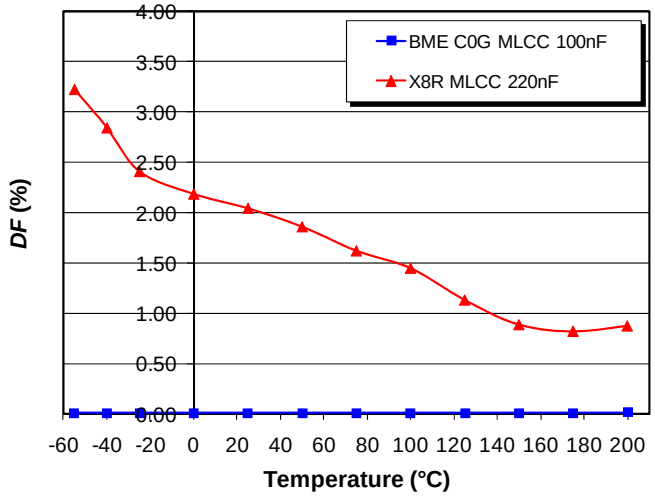

Fig. 6. *DF* dependence on temperature without DC bias.

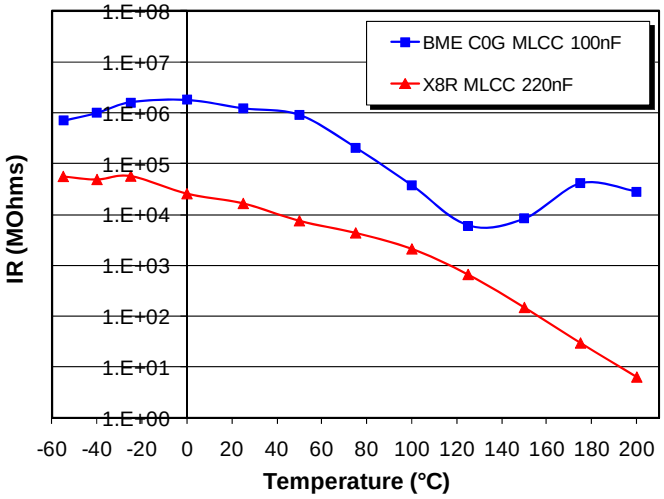

Fig. 7. IR dependence on temperature with 25V DC bias.

The dielectric breakdown strength of the BME C0G and X8R MLCC samples was also investigated, and results are shown in Fig. 8. From room temperature to 150°C, the breakdown strength of BME C0G MLCC only dropped from 233 Volts/µm to 207 Volts/µm, while that for the X8R MLCC dropped from 103 Volts/µm to 55 Volts/µm, which was a reduction of 46%. At 150°C, the breakdown strength of BME C0G MLCC is 3.7 times higher than the X8R MLCC. Breakdown test for X8R MLCC could not be conducted at temperatures above 150°C due to its high leakage.

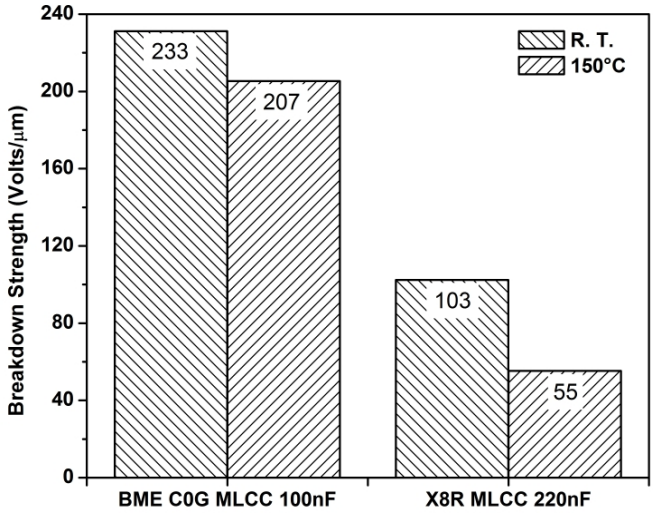

Fig. 8. Dielectric breakdown strength at room temperature and 150°C.

4. Lifetime Prediction at High Temperatures

One of the key parameters for high temperature applications is the long term reliability. As reported earlier [6, 7], unlike the typical $BaTiO_3$ based BME X7R/X5R dielectric materials, oxygen vacancy is not a concern for reliability in BME C0Gs based on $CaZrO_3$. In order to estimate the lifetime in high temperatures applications, a highly accelerated life test (HALT) study was used. The HALT data under various temperature and voltage conditions was used to extrapolate the reliability of the capacitor at typical use conditions. The detailed principle and procedures of this kind of study have been well reported [11-13], and will be only summarized in this paper. An empirical equation by Prokopowicz and Vaskas (P-V equation), shown in equation (2), is employed to correlate the reliability behavior under accelerated test conditions to operating conditions.

$$\frac{t_1}{t_2} = \left(\frac{V_2}{V_1}\right)^n \exp\left[\frac{E_a}{k}\left(\frac{1}{T_{1_{abs}}} - \frac{1}{T_{2_{abs}}}\right)\right] \tag{2}$$

where:

t_i = time to failure under conditions i,
V_i = voltage under condition i,
n = voltage stress exponential,
E_a = activation energy for dielectric wear out,
k = Boltzmann's constant (8.62×10^{-5} eV/K),
T_i = absolute temperature for condition i.

The P-V equation can be simplified to equation (3):

$$t = A\frac{1}{V^n}\exp\left(\frac{E_a}{kT}\right) \tag{3}$$

where A is the time constant. Equation (3) can also be put into the following natural log form for easy experimental data multi-regression.

$$Ln[t] = Ln[A] - n\,Ln[V] + \frac{E_a}{kT} \tag{4}$$

Typically the time (t) used for reliability modeling is the median time to failure (MTTF). By running HALT at multiple combinations of voltages and temperatures, the median time to failure data at each combination can be obtained from the time-to-failure data distribution fitting if more than 50% of the parts failed during testing. Using the multi-regression tool in a commercial software package, parameters such as A, n, and E_a can be determined. Thus, from equation (3), a lifetime can be predicted under given use conditions (voltage V and temperature T).

Three BME C0G MLCC part types, 0402-101-50V, 0603-471-50V and 0805-222-50V were tested under HALT conditions at 4 temperatures (125°C, 150°C, 175°C, and 200°C) and 6 voltages (300V, 400V, 450V, 500V, 550V, and 600V) for 200 hours. The maximum temperature (200°C) and maximum voltage (600V) used in this study were limited by the equipment capability. A sample size of 20 pieces was used in each HALT run. HALT time-to-failure (TTF) was recorded when IR at test temperature dropped below 4.28 MΩ.

Figure 9 shows the HALT time-to-failure distributions for part type 0805-222-50V under various temperature and voltage conditions. Following the steps described above, a time constant A, voltage exponential n, and the activation energy E_a were obtained by multi-regression and are listed in Table I. The R-Sq. of this regression was 94.7%. By substituting values of A, n and E_a parameters back into equation (3), MTTF can be calculated for various use conditions. Some of these use conditions are listed in Table II as examples. At 150°C and 50V, the predicted lifetime is over 52.6 million years, and even at 200°C and 50V, the predicted median lifetime is 1.48 million years.

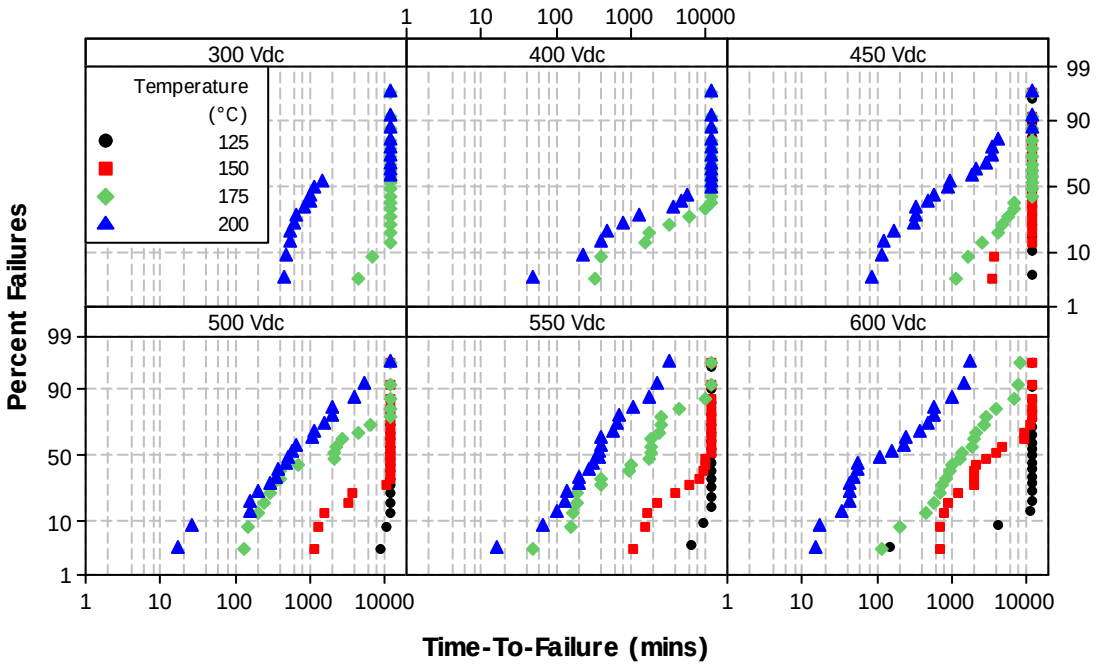

Fig. 9. HALT distributions at various test conditions for 0805-222-50V.

Table I. Multi-regression Results for HALT-TTF P-V Model for 0805-222-50V

Part Type	A (mins)	n	*E*a (eV)	R^2
C0805C222J5GAB	1.30E+14	9.0	1.23	94.7%

Table II. Lifetime Prediction from MTTF Model for 0805-222-50V

Part Type	CAP (nF)	Rated Voltage	Application Temperature (°C)	Application Voltage	MTTF (Years)
C0805C222J5GAB	2.20	50	25	50	7.47E+13
				25	3.91E+16
			125	50	4.39E+08
				25	2.29E+11
			150	50	5.26E+07
				25	2.75E+10
			175	50	7.98E+06
				25	4.17E+09
			200	50	1.48E+06
				25	7.73E+08

The HALT-MTTF data of each combination of the temperature and voltage for the part types 0402-101-50V and 0603-471-50V is summarized in Table III. As shown in Fig. 10, there were not enough failures under even the most severe HALT conditions used up to 200hrs of test time. While this is a strong proof of the robust reliability of these BME C0G capacitors under the accelerated test conditions, these tests still could not cause the required number of failures (50^{th} percentile) needed to model the median-time-to-failure (MTTF) data. Thus, their HALT distribution fitting can not be performed. This also indicates that it is not necessary to de-rate the voltage rating for the BME C0G MLCC tested in this study for high temperature applications, which is a clear advantage over the MLCCs based on X7R/X8R dielectrics.

Table III. MTTF Data for 0402-101-50V and 0603-471-50V (N. E. F. = Not Enough Failures)

MTTF (mins)		Temp (°C)			
	Volts	125	150	175	200
C0402C101J5GAB	300	Not Tested	Not Tested	N. E. F.	N. E. F.
	400	Not Tested	Not Tested	N. E. F.	N. E. F.
	450	N. E. F.	N. E. F.	N. E. F.	N. E. F.
	500	N. E. F.	N. E. F.	N. E. F.	N. E. F.
	550	N. E. F.	N. E. F.	N. E. F.	N. E. F.
	600	N. E. F.	N. E. F.	N. E. F.	N. E. F.

MTTF (mins)		Temp (°C)			
	Volts	125	150	175	200
C0603C471J5GAB	300	Not Tested	Not Tested	N. E. F.	N. E. F.
	400	Not Tested	Not Tested	N. E. F.	N. E. F.
	450	N. E. F.	N. E. F.	N. E. F.	N. E. F.
	500	N. E. F.	N. E. F.	N. E. F.	N. E. F.
	550	N. E. F.	N. E. F.	N. E. F.	N. E. F.
	600	N. E. F.	N. E. F.	N. E. F.	N. E. F.

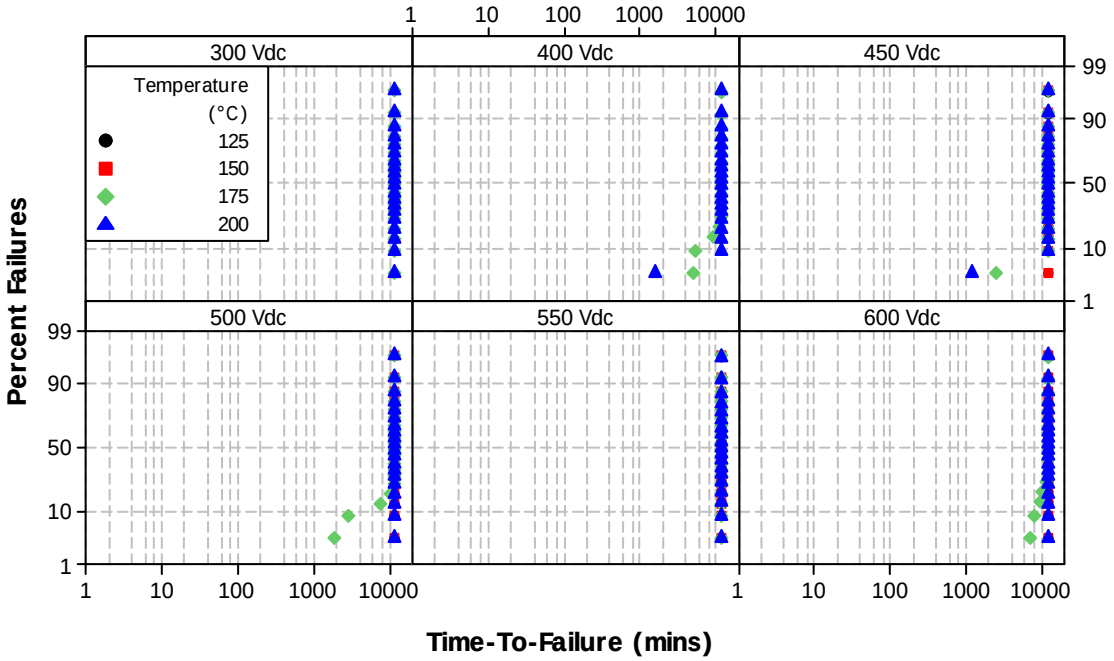

Fig. 10. HALT distributions at various test conditions for 0603-471-50V.

5. Summary

1. The $CaZrO_3$ based BME C0G dielectric material shows robust performance for high temperature applications. At temperature up to 200°C, it meets the EIA X9G specification (capacitance variation from the reference point of 25°C should be within 0 ± 30 ppm/°C (or $\Delta C_{Max}/C \leq 0.525\%$) over the temperature range of –55°C to +200°C) and exhibits good long term reliability.

2. The $CaZrO_3$ based BME C0G MLCCs exhibit good potential for energy storage applications even when used at temperatures above 150°C. This is complimented by their stable dielectric constant, low dielectric losses, high IR, high breakdown strengths and good reliability at high temperatures.

3. Traditional $BaTiO_3$-based X8R dielectrics suffer from severe capacitance reduction, insulation resistance deterioration, and breakdown voltage reduction at high temperatures above 150°C. Thus, their nominal capacitance and the voltage rating should be carefully investigated if applications involve temperatures above 150°C.

6. References

[1] E. F. Alberta, et al., "High Temperature Ceramic Multilayer Capacitors," p69-72, *Proceedings of the 24th Symposium for Passive Components (CARTS USA 2004)*, San Antonio, TX, USA, 2004.

[2] C. J. Stringer, et al., "New Relaxor Dielectrics for High Temperature Capacitors," p381-384, *Proceedings of the 12th US-Japan Seminar on Dielectric and Piezoelectric Ceramics*, Annapolis, Maryland, USA, 2005.

[3] E. F. Alberta, et al., "High Temperature Ceramic Capacitors," p471-477, International Conference and Exhibition on High Temperature Electronics (HiTEC 2006), Santa Fe, NM, Mexico, USA, 2006.

[4] W. Schulze, et al., "High Temperature Capacitor - Sodium Bismuth Titanate – Idea to Application," p478-484, International Conference and Exhibition on High Temperature Electronics (HiTEC 2006), Santa Fe, NM, Mexico, USA, 2006.

[5] http://www.epcos.com/inf/20/10/ds/MLSC.pdf.
[6] X. Xu, et al., "High CV BME C0G," p179-188, *Proceedings of the 27th Symposium for Passive Components (CARTS USA 2007)*, Albuquerque, NM, USA, 2007.
[7] A. Gurav, et al., "Characteristics of $CaZrO_3$-Based BME C0G Dielectric," p359-362, *Proceedings of the 13th US-Japan Seminar on Dielectric and Piezoelectric Ceramics*, Awaji Island, Hyogo, Japan, 2007.
[8] N. H. Fletcher, et al., "Optimization of Energy Storage Density in Ceramic Capacitors," *J. Phys. D: Appl. Phys.*, 29, 253-258 (1996).
[9] M. D. Waugh, et al., "Structure-Property Investigation of a Modified $PbHfO_3$ Composition for High Energy Storage", p153-163 in Ceramic Transactions, Vol. 90, *Manufacturing of Electronic Materials and Components*, The American Ceramic Society, 1998.
[10] X. Xu, et al., "Advances in Class-I C0G MLCC and SMD Film Capacitors," p449-461, *Proceedings of the 28th Symposium for Passive Components (CARTS USA 2008)*, Newport Beach, CA, USA, 2008.
[11] T. Prokopowicz and A. Vaskas, "Research and Development, Intrinsic Reliability, Subminiature Ceramic Capacitors," Final Report, ECOM-9705-F, 1969 NTIS AD-864068.
[12] J. L. Paulsen, et al., "Highly Accelerated Life Testing of KEMET Base Metal Electrode (BME) Ceramic Chip Capacitors," p265-270, CARTS 2001.
[13] T. Ashburn, et al., "Highly Accelerated Testing of Capacitors for Medical Applications ," *Proceedings of the 5th SMTA Medical Electronics Symposium*, Anaheim, CA, USA, 2008.